 MCB, vol.5, no.2, pp.119-132, 2008

Development of a Gastrointestinal Tract Microscale Cell Culture Analog to Predict Drug Transport

Gretchen J. McAuliffe*, Jung Yun Chang†, Raymond P. Glahn‡ and Michael L. Shuler§

Abstract: Microscale cell culture analogs (μCCAs) are used to study the metabolism and toxicity of a chemical or drug. These *in vitro* devices are physical replicas of physiologically based pharmacokinetic models that combine microfabrication and cell culture. The goal of this project is to add an independent GI tract μCCA to a multi-chamber chip μCCA representing the primary circulation. The GI tract μCCA consists of two chambers separated by a microporous membrane on which intestinal epithelial cells are cultured. Compounds of interest are pumped through the top chamber, allowing drug to be absorbed through the epithelial layer and circulated into the chip μCCA. The chip and GI tract μCCAs have been used to recreate the toxic effects of acetaminophen. Preliminary results have shown that the GI tract μCCA acts as a barrier to drugs entering the chip, mimicking *in vivo* function in this regard.

1 Introduction

The cost of developing a new drug was recently estimated to be 1.9 billion dollars [1]. With the majority of drug candidates failing in expensive phase III clinical trials, there is a significant economic need for a method that accurately assesses the ADMET (absorption, distribution, metabolism, elimination, and toxicity) of drug candidates early in the development process [2]. *In vitro* cell cultures and animal models are the two most common methods used to determine toxicological and pharmacological profiles of potential drugs, but both methods have disadvantages. The largest problem with single cell type, monolayer cell cultures is that the effects of drug metabolites and systemic changes caused by the compound of interest cannot be studied [3]. Animal experiments can take months to complete, cost millions of dollars, and the majority of drugs shown to be safe in animals fail in human clinical trials [3].

This work describes an *in vitro* system that may be able to better predict animal or human response to oral drug exposure. A cell culture analog (CCA) can be defined as a physical representation of a physiologically based pharmacokinetic (PBPK) model. A PBPK mathematical model describes an organism as a set of interconnected compartments that are based on vasculature structure, and is designed to describe the time-dependent distribution of a chemical or drug in various tissues [4]. The CCA devices consist of channels and chambers arranged and sized to mimic the residence time and flow distribution of the corresponding PBPK model. In addition, where the PBPK model mathematically specifies an organ or tissue compartment, the CCA has an actual chamber holding a cell type that mimics the organ or tissue. Recirculating culture medium represents the circulatory system. The goal of a CCA is to create an *in vitro* system that can replicate some of the cell-cell interactions (i.e. interactions through soluble proteins and metabolites) in humans or animals not easily studied *in vivo* or *in silico* and to apply these observations to toxicology studies.

* School of Chemical and Biomolecular Engineering, Cornell University, Ithaca, New York 14853, USA

† Korea Food and Drug Administration, Seoul, Korea

‡ Plant, Soil and Nutrition Laboratory, Agricultural Research Services, U.S. Department of Agriculture, Tower Road, Ithaca, NY 14853, USA

§ Department of Biomedical Engineering, Cornell University, Ithaca, New York 14853, USA. Corresponding author. Cornell University, Department of Biomedical Engineering, 120 Olin Hall, Ithaca, NY 14853, USA. Tel: (607)255-7577; Fax: (607)255-9166; E-mail: mls50@cornell.edu (M.L. Shuler)

A three-chamber (lung, liver, and other tissues) microscale cell culture analog (μCCA) has been developed using tools from the semiconductor industry [5]. The μCCA consists of etched cell compartments connected by channels on a 2.5 cm x 2.5 cm silicon chip, with culture medium recirculated through the chip using a peristaltic pump. A four-chamber (lung, liver, fat, and other tissues) μCCA was used to demonstrate the effects of naphthalene on various tissues [6]. Two chambers (lung and liver) contained living cells; the other tissue and fat compartments had no cells, but mimicked the distribution of fluid in rapidly and slowly perfused tissues. Naphthalene added to the circulating culture medium was converted to reactive metabolites in the liver compartment. When these metabolites circulated to the lung compartment the concentration of glutathione, a protective compound, was reduced in the lung cells, resulting in lung cell death. In control experiments without liver cells, however, there was no lung cell death. Later experiments using adipocyte-like cells in the fat chamber showed how fat could modify the response [7]. These experiments show that the system can recreate the known effects of a toxic chemical. The microscale size of the device allows for near *in vivo* organ residence times, fluid to tissue ratios, and cellular shear stress values. The small size also decreases manufacturing costs, reagent amounts, and space needed.

In the proof of concept, four-chamber chip, test chemicals were added directly to the circulating culture medium, which mimics intravenous administration of a compound. The purpose of this work is to connect an independent gastrointestinal (GI) tract μCCA to a three-chamber "body" chip μCCA, which may provide a superior *in vitro* method for testing the ADMET of orally administered pharmaceuticals. The GI tract μCCA consists of two chambers mounted on top of each other and separated by a microporous membrane, on which intestinal epithelial cells are cultured. The top or apical chamber represents the intestinal lumen, and the bottom or basolateral chamber represents the capillary network surrounding the intestinal tract. **Figure 1** shows a photograph and side-view schematic of the GI tract μCCA. The separate GI tract unit will be referred to as the GI tract μCCA, the silicon "body" chip will be referred to as the chip μCCA, and the connected GI tract and chip μCCAs will be referred to as the μCCA system.

Acetaminophen (APAP) was chosen as a model drug for this work. APAP toxicity is closely linked to GI and liver cell metabolism of the drug. Therapeutic doses are primarily metabolized by phase II conjugation with sulfate and glucuronide [8]. Approximately 5-10% of a therapeutic APAP dose is oxidized by cytochrome P450 (CYP) 1A1/2, 2E1, or 3A4 to *N*-acetyl-*p*-benzoquinone (NAPQI), a toxic, electrophilic metabolite [9, 10]. NAPQI is detoxified by conjugation with glutathione via glutathione-*S*-transferase and excreted in urine or bile [11]. Large doses of APAP that overwhelm the sulfation and glucuronidation pathways or the induction of CYP enzymes with drugs such as ethanol can result in high levels of NAPQI [8]. High levels of NAPQI cause glutathione depletion and eventual NAPQI accumulation; NAPQI electrophilically attacks proteins in nearby cells and causes cell death [12].

In these proof of concept experiments, APAP was used to test the hypothesis that drug passes through the intestinal epithelial monolayer in the GI tract μCCA, circulates to the liver and lung compartments on the chip μCCA, and causes glutathione depletion and cell death. A four-compartment model was used where lung, liver, and other tissues compartments were etched into silicon chips and the GI tract was a separate device fabricated from plexiglass. Three of the chambers (lung, liver, and GI) contain cells, while the other tissues compartment only mimics the distribution of fluid in slowly perfused tissues.

2 Materials and Methods

Materials. Dulbecco's Modified Eagle Medium (DMEM), Minimum Essential Medium (MEM), Dulbecco's Modified Eagle Medium:Nutrient Mix F-12 (DMEM/F12, 1:1), fetal bovine serum (FBS), trypsin-EDTA (0.25%), phosphate buffered saline (PBS), calcein, and monochlorobimane (MCB) were obtained from Invitrogen (Grand Island, NY). Polycarbonate, 0.4 μm pore

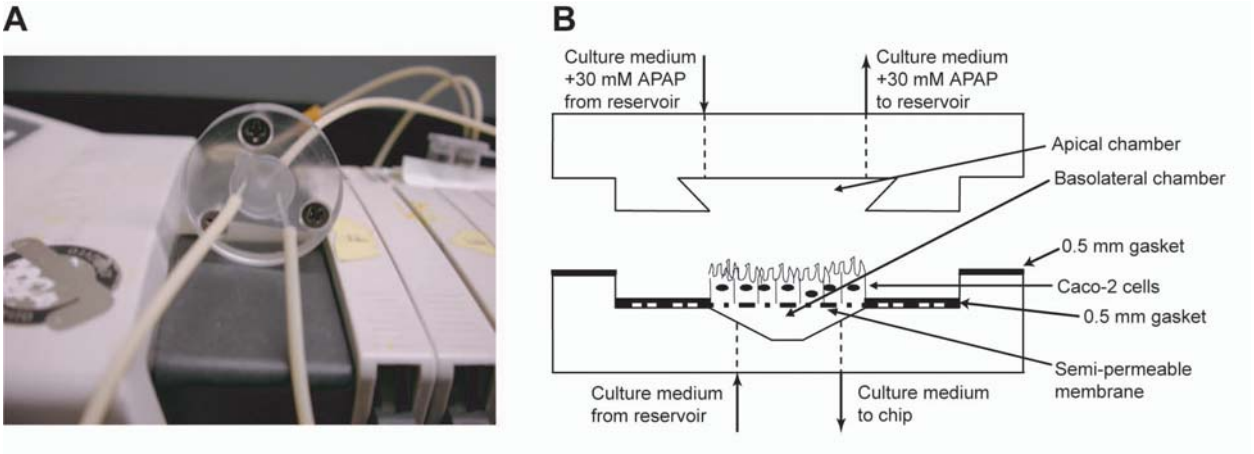

Figure 1: (A) Photograph of the apical side of the GI tract μCCA. (B) A side-view schematic of the GI tract μCCA. The dimensions of the apical and basolateral chambers are as follows (diameter of the top of the chamber $\times$ height $\times$ diameter of the bottom of the chamber): apical chamber (8 mm $\times$ 0.8 mm $\times$ 2.8 mm) and basolateral chamber (2.8 mm $\times$ 0.8 mm $\times$ 0.8 mm). The total area of Caco-2 cells exposed to flow was 6.2 mm^2.

size membranes were obtained from Whatman Inc. (Florham Park, New Jersey). Membranes were coated with Type I collagen from Becton Dickinson (Bedford, MA). Human plasma fibronectin was acquired from Millipore (Billerica, MA). Clear, 96 well and 6 well assay plates were purchased from Corning Life Sciences (Corning, NY). β-glucuronidase/arylsufatase was purchased from Roche Applied Science (Indianapolis, IN). Silicone wafers were purchased from Silicon Quest (Santa Clara, CA). P20 primer and Shipley 1813 and 1027 photoresist were purchased from Shipley Company (Marlborough, MA). MIF 300 developer was obtained from Clariciut (Somerville, NY). Unless otherwise stated, all other chemicals were purchased from Sigma Aldrich (St. Louis, MO).

Cell culture. The Caco-2 (human colon carcinoma), HepG2/C3A (human hepatocellular carcinoma) and L2 (rat lung) cell lines were obtained from the American Type Culture Collection (Manassas, VA). Caco-2 cells were received at passage 17; used in experiments at passage 30-35; and cultured in DMEM with 4.5 g/L glucose, 25 mM HEPES buffer, 4 mM L-glutamine, and 10% FBS. HepG2/C3A cells were maintained in MEM with 1.0 mM sodium pyruvate and 10% FBS. L2 cells were cultured in DMEM/F12 with 10% FBS.

Cytochrome P450 1A and 2E1 Measurement. CYP1A activity was measured using the method described by Donato et al. [13]. HepG2/C3A cells were seeded at 250,000 cells/cm^2 in clear 96 well plates coated with 8 μg/cm2 fibronectin and grown for 48 hours. Caco-2 cells were seeded at 100,000 cells/cm^2 in clear 96 well plates coated with 8 μg/cm^2 Type I collagen and grown for 16 days. Cells were then washed twice with PBS and 100 μL of assay medium, which consisted of phenol red-free DMEM/F12 containing 8 μM ethoxyresorufin and 10 μM dicumerol, was added to each well. After a 1 hour incubation at 37°C and 5% CO_2, 75 μL of assay medium was taken from each well and transferred to a separate 96 well plate; subsequently 15 Fisherman units of β-glucuronidase and 120 Roy units of arylsulfatase in 25 μL in 0.1 M sodium acetate buffer (pH 4.5) were added to each well containing 75 μL assay medium. The 96 well plates were then incubated at 37°C for 2 hours, 200 μL of ethanol was added to each well, and the plates were centrifuged at 3000 rpm for 10 minutes. The amount of resorufin formed and released into the culture medium was quantified at 530 nm excitation and 590 nm emission by a SpectraMax Gemini EM fluorescence microplate reader from Molecular Devices (Sun-

nyvale, CA). A standard curve for resorufin was prepared in phenol red free DMEM/F12 and processed in the same manner as samples.

CYP2E1 activity was assessed using the methods described by Donato et al. and Dicker et al. [14, 15]. HepG2/C3A cells were seeded at 250,000 cells/cm^2 in clear 96 well plates coated with 8 μg/cm^2 fibronectin and grown for 48 hours. Caco-2 cells were seeded at 100,000 cells/cm^2 in clear 96 well plates coated with 8 μg/cm^2 Type I collagen and grown for 16 days. Cells were then washed twice with PBS and 100 μL of assay medium, which consisted of phenol red-free DMEM/F12 containing 500 μM *p*-nitrophenol, was added to each well. After a 1 hour incubation at 37°C and 5% CO_2, 75 μL of assay medium was taken from each well and transferred to a separate 96 well plate. 15 Fisherman units of β-glucuronidase and 120 Roy units of arylsulfatase in 25 μL in 0.1 M sodium acetate buffer (pH 4.5) were added to each well containing 75 μL assay medium. The 96 well plates were incubated at 37°C for 2 hours and then 10 μL of 10 M NaOH was added to each well. The amount of *p*-nitrophenol hydroxylation to 4-nitrocatechol was quantified by measuring the sample absorbance at 546 nm with a VersaMax^{TM}microplate reader (Molecular Devices). A standard curve for 4-nitrocatechol was prepared in phenol red free DMEM/F12 and processed in the same manner as samples.

Following the CYP1A and CYP2E1 assays the total cell protein was measured using the Bradford method described by Kautzky et al. [16, 17]. The remaining 25 μL of assay medium was removed from the cells and the monolayers were washed twice with PBS. The cells were then lysed by adding 50 μL of 0.1 M NaOH and incubating for 1 hour at room temperature. After lysing the cells, 200 μL of Bradford reagent was added to each well and absorbance was read at 595 nm with a microplate reader. Dilutions of 0 to 1 mg/mL bovine serum albumin (BSA) dissolved in 0.1 M NaOH were used as protein standards.

μCCA Fabrication. The chip μCCA was fabricated at the Cornell Nanofabrication Facility (CNF) using standard photolithography and etching techniques that have been described previously [5]. The chip pattern was first designed on CAD (Cadence, Fishkill, NY). The pattern was then converted onto a chrome-coated glass mask via the 3600F optical pattern generator (D.W. Mann/GCA Corp., USA). Two masks were required for the two layers of fabrication, a 40 μm etch and a 100 μm etch.

A 4.00 inch diameter, 525 μm thick, <100>, silicon wafer was primed with P20 primer at 3000 rpm for 30 seconds. Next, the wafer was coated with 1.3 μm of Shipley 1813 photoresist at 3000 rpm. The first mask pattern was transferred to the wafer with UV light (405 nm) for 2.5 seconds using an AB-M HTG 3HR Contact Proximity Aligner (San Jose, CA). The wafer was then developed for 1 minute in MIF 300 developer, rinsed in DI water, and dried. A UNAXIS 770 plasma etcher (Unaxis USA Inc., St. Petersburg, FL) was used to etch the wafer at a rate of approximately 2 μm/min to a depth of 40 μm.

For the second layer of fabrication the wafer was once again primed with P20 primer before Shipley 1075 photoresist was spun on the wafer at 2000 rpm for 30 seconds. The second mask pattern was transferred to the wafer with UV light for 30 seconds using the HTG contact aligner. The wafer was again developed and etched with the UNAXIS 770 to a depth of 100 μm. Finally, the wafer was stripped using a heated resist bath and the individual chips (7 per wafer) were separated by scoring with a diamond blade and breaking the wafer. **Figure 2** is a photograph of the chip μCCA used for these experiments.

The GI tract μCCA was fabricated from 1/2 thick plexiglass (McMaster-Carr, New Brunswick, NJ) by Glenn Swan (School of Chemical and Biomolecular Engineering, Cornell University). A photograph and side-view schematic of the GI tract μCCA are shown in **Figure 1**. The plastic was etched so that the top piece contained a chamber that was 8 mm at the top (surface where the fluid inlet and outlet are located), 0.8 mm high, and 2.8 mm at the bottom (the surface that comes in contact with the cell monolayer). The bottom piece had an etched chamber that was 0.8 mm at the bottom (surface where the fluid inlet and

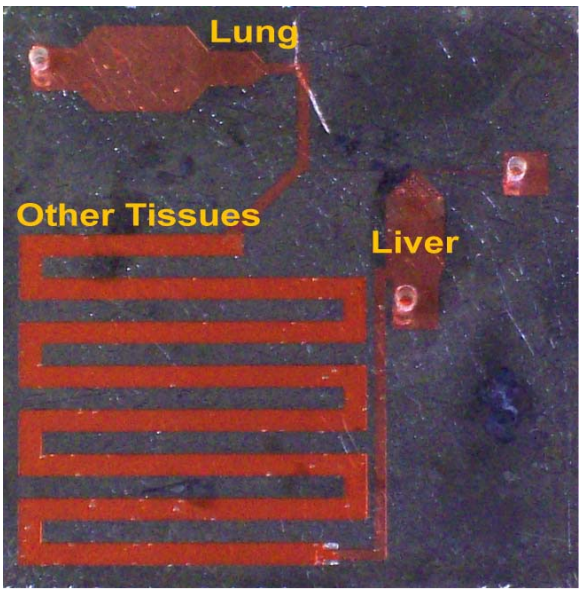

Figure 2: A photograph of the chip μCCA. The dimensions of the chambers are as follows (w $\times$ l $\times$ d): lung (2 mm $\times$ 1.6 mm $\times$ 40 μm), liver (2 mm $\times$ 6 mm $\times$ 40 μm), and other tissues (1 mm $\times$ 123 mm $\times$ 100 μm). The channels connecting compartments were 100 μm deep. The chip was designed so 85% and 15% of the medium leaving the lung compartment goes to the other tissues and liver chambers, respectively, while 100% of medium leaving the basolateral GI tract μCCA chamber goes to the liver.

outlet are located), 0.8 mm high, and 2.8 mm at the top (the surface that comes in contact with the cell monolayer). The top and bottom pieces had two-step inlet and outlet channels drilled with a diameter of 740 μm (drill size number 69, Small Parts Inc., Miami Lakes, FL) for the top half of the channel and 610 μm (drill size number 73, Small Parts) for the bottom half of the channel.

μCCA Toxicity Experiments. The bottom chambers of the GI tract μCCAs were first sterilized by soaking for 30 minutes in 70% EtOH and then placed in a 6 well plate. Polycarbonate, 0.4 μm pore size membranes were cut to 12 mm in diameter, sterilized by autoclaving in a dry cycle for 30 minutes, and placed in the bottom chamber. A sterile, 12 mm outer diameter (OD), 10 mm inner diameter (ID), 0.5 mm thick, silicone gasket was placed over the membrane (Grace Bio-Labs, Bend, OR, gasket was cut to the correct size from a silicone sheet). The membrane and gasket were held in place with a 12 mm OD, 10 mm inner diameter (ID) sterile washer. The membranes were coated with 8 μg/cm^2 Type I collagen dissolved in 0.02 M acetic acid for 1 hour and then washed with the same volume of PBS. Caco-2 cells were seeded onto the membranes at a concentration of 100,000 cells/cm^2, allowed to attach for 2 hours at 37°C and 5% CO_2, and then each well of the 6 well plate was filled with 3 mL DMEM. Caco-2 cells were grown on the membrane for 16 days prior to experiments to allow for full coverage of the membrane and cell differentiation.

μCCA chips were cleaned with a solution of 70% sulfuric acid and 30% hydrogen peroxide (30% H_2O_2 solution) for 10 minutes at room temperature and then rinsed with DI water. After cleaning, 1 mm thick silicone gaskets (Grace Bio-Labs) with holes cut out over the cell chambers were placed onto the chips to keep coating and cell suspensions within the proper compartments. The chips with gaskets over them were dried in an oven at 60°C for 30 minutes to seal the two together, and then both were autoclaved in a dry cycle for 30 minutes.

The μCCA chips were first coated with 4 μg/cm^2 poly-D-lysine in PBS for 5 minutes at room temperature. The poly-D-lysine solution was removed from each chamber and each chamber was washed with an equal volume of PBS. The chips were then coated with 8 μg/cm^2 fibronectin in PBS for 1 hour at room temperature. The fibronectin solution was removed, L2 cells were seeded into the lung chamber at a concentration of 200,000 cells/cm^2, and HepG2/C3A cells were seeded into the liver chamber at a concentration of 250,000 cells/cm^2. The chips were kept at 37°C and 5% CO_2 for 4 hours to allow the cells to attach and then the Petri dish holding the chips was filled with 25 mL of DMEM/F12. Cells were grown for 48 hours before toxicity experiments.

On the day of the toxicity experiments, autoclaved, 0.25 mm ID diameter, Pharmed peristaltic pump tubing (Cole-Parmer, Vernon Hills, IL) was placed into a peristaltic pump (205S, Wat-

son Marlow, Wilmington, MA) and DMEM/F12 was pumped at 10 rpm through the tubing to remove air bubbles. Tips from 200 μL gel loading tips (Fisher Scientific, Hampton, NH) were inserted into the ends of the peristaltic pump tubing and these tips fit securely into the inlet and outlet holes of the top and bottom pieces of the GI tract μCCA and plexiglass housing around the chip μCCA.

The GI tract μCCAs were assembled by placing a 0.5 mm thick gasket on the outer edge of the bottom piece and screwing the top and bottom pieces together tightly with the membrane holding Caco-2 cells in between the two pieces. The pump flow rate was decreased to 0.75 rpm or approximately 3.5 μL/min, and tubing from one pump channel was used for the GI tract μCCA apical or top inlet and tubing from a second pump channel was used for the basolateral or bottom inlet. Once culture medium could be seen exiting the outlet channels on the apical and basolateral sides, tubing was also connected to the outlet channels. Medium was pumped through the GI tract μCCAs during chip assembly ($\sim$1 hour) to rid the devices of air bubbles.

The silicone gaskets were peeled off the top of the chips and the chips were then placed between two pieces of 1/8" thick machined plexiglass that were screwed together tightly. The top pieces of plexiglass had two-step inlet and outlet holes (740 μm for the top half and 610 μm for the bottom half) and were cleaned with 70% EtOH and treated with oxygen plasma in an Expanded Plasma Cleaner (Harrick Plasma, Ithaca, NY) for 1 minute before assembly to increase surface wettability and sterility [18]. The bottom pieces of plexiglass were etched with $\sim$1.5 mm deep chambers that were slightly larger than the chips. A 1 mm thick piece of silicone gasket (Grace Bio-Labs) was placed into each of these cavities to allow for a tight seal between the top piece of plexiglass, chip, and bottom plexiglass piece. The bottom piece was sterilized by soaking in 70% EtOH for 30 minutes prior to assembly. After removing the silicone gasket from a chip, it was placed into the bottom plexiglass piece and 200 μL of MEM was pipetted on top of the chip. When pipetting MEM onto the chips, care was taken to remove any air bubbles in the liquid and to keep the liquid from spilling off of the chip and into the plexiglass chamber. The top plexiglass piece was then lowered straight down onto the chip, and the top and bottom pieces were screwed together.

After the chips were assembled, the outlet tubing from the basolateral side of the GI tract μCCA was connected to the liver inlet of the chip. Tubing from a third pump channel was attached to the lung inlet. 23-gauge, stainless steel needles were inserted into the tubing starts and ends. These needles were inserted into a well from an 8 well strip plate (Corning) sealed with a silicone cover (996050MR, BioTech Solutions, Mt. Laurel, NJ), which acted as a 200 μL culture medium reservoir and debubbler. The basolateral side of the GI tract μCCA and chip shared one reservoir that contained only DMEM/F12. The apical side of the GI tract μCCA had a different reservoir that contained DMEM/F12 only (control) or DMEM/F12 +30 mM APAP. The experimental set-up is shown in **Figure 3**.

The system was operated at 37°C and 5% CO_2 for 6 hours. At the end of the experiments, cells were stained with calcein, a viability stain, and MCB, a glutathione (GSH) stain. DMEM/F12 containing 5 μM calcein and 80 μM MCB was circulated through the GI tract and chip μCCAs for 30 minutes at 37°C.

Fluorescence Microscopy and Image Analysis. Fluorescent images were acquired with a Retiga CCD camera (Qimaging, Burnaby, BC, Canada) mounted to an Olympus BX51 microscope (Olympus America Inc., Center Valley, PA) with a 10X objective. The microscope and camera were connected to a computer running the Image Pro Plus version 4.6 software package (Media Cybernetics Inc., Silver Springs, MD) in 12-bit grayscale format. Fluorescence from the calcein stain was collected with an EGFP cube (Ex 470/Em 610, Chroma Technology Corp., Rockingham, VT). Fluorescence from the MCB-GSH adduct was collected with a DAPI cube (Ex 360/Em 460). Both image types (calcein, MCB-GSH) were obtained in the same field of view; 2 images were taken for each lung compartment

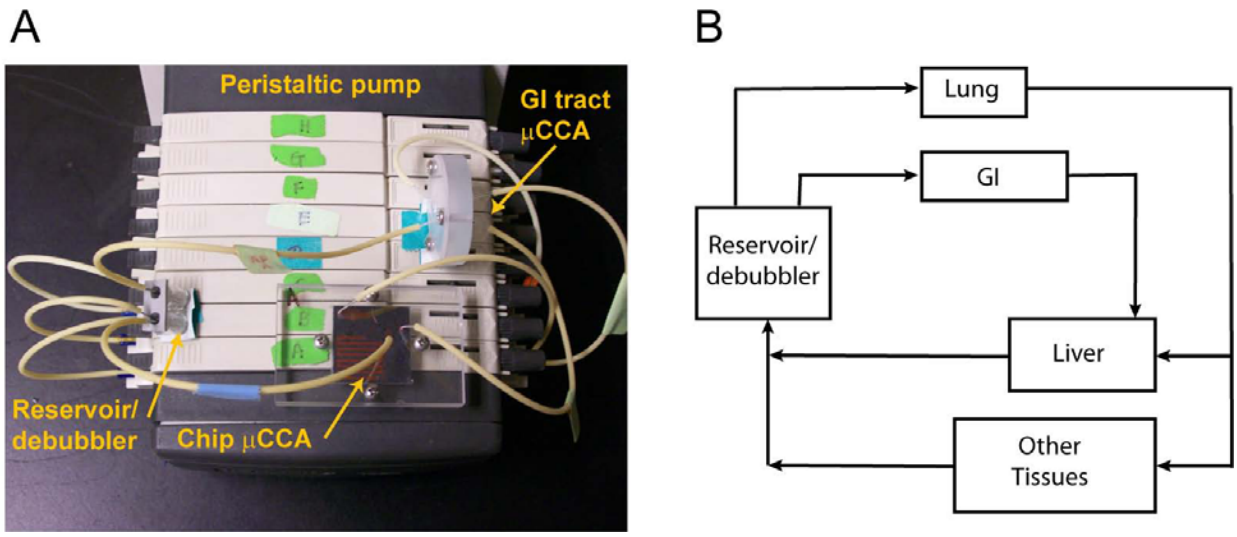

Figure 3: (A) Photograph of the μCCA system experimental set-up and (B) a PBPK schematic of the flow pattern through the μCCA system.

and 6 images were taken from each liver compartment. Images were analyzed for total area stained with Image Pro Plus software.

HPLC. APAP concentration in experimental culture medium was determined using the protocol described by Wang et al. [19]. Briefly, samples taken from the culture medium reservoirs were extracted with an equal volume of acetonitrile and centrifuged at 3,000 rpm for 10 minutes. A 100 μL injection of the supernatant was used for determination of APAP by reverse-phase HPLC analysis. A Waters 2690 separations module and Waters 996 photodiode array detector set at a wavelength of 254 nm were used (Waters Corporation, Milford, MA). Chromatogram analysis was performed using Millennium software (version 3.0, Waters). Separations were done on a 250 x 4.6 mm, RP18, 5 μm XTerra column (Waters). APAP was eluted with 7% acetonitrile (v/v in water) with 0.1% trifluoroacetic acid (v/v) at a flow rate of 1.8 mL/min. Comparison with standards was used for identification and quantification.

Statistical Analysis. Results are expressed as mean $\pm$ standard error. Data was analyzed with the GraphPad Prism version 4.00 for Windows (GraphPad Software, San Diego, CA). An unpaired Students's t-test was used for data analysis. Differences were considered significant at $p < 0.05$.

3 Results

Design of the μCCAs. **Figure 3** shows a photograph of the connected chip and GI tract μCCAs. Three channels were used on the peristaltic pump for the two devices. The first channel pumped DMEM/F12 or DMEM/F12 +30 mM APAP through the apical chamber of the GI tract μCCA at $\sim$3.5 μL/min. After the medium passed through the apical chamber of the GI tract μCCA, it returned to a reservoir containing 200 μL of DMEM/F12 or DMEM/F12 +30 mM APAP. The second channel pumped DMEM/F12 at $\sim$3.5 μL/min into the lung chamber. After the culture medium passed through the lung chamber, 85% of the liquid went to the other tissues chamber and 15% went to the liver chamber. The third pump channel was used to pump liquid at $\sim$3.5 μL/min into the basolateral side of the GI tract μCCA. All liquid from the basolateral outlet of the GI tract μCCA then went through a second inlet to the liver chamber, mimicking first pass metabolism. The culture medium from the liver and other tissues chambers combined at the chip outlet and returned to a second reservoir containing 200 μL DMEM/F12 before being recirculated to the lung and basolateral GI tract inlets. **Table 1** compares the physiological parameter values for rat with those of the μCCAs. The chip chambers

Table 1: Comparison between rat physiological parameter and μCCA design parameter values for the μCCA system. Values for rat body weight, regional blood flow distribution, and organ residence times were taken from Brown et al. [4]. GI flow rates for the μCCA represent flow through the basolateral GI tract μCCA chamber.

Tissue	% Body weight (rat)	% Cardiac output (rat)	Residence time (s)
GI	2.7%	14%	26
Lung	0.50%	100%	1
Liver	3.4%	18%	27
Other	96%	82%	186

Tissue	% μCCA compartment volume	% Medium flow (μCCA)	Residence time (s)
GI	2.3%	100%	5
Lung	0.98%	100%	2
Liver	3.6%	115%	7
Other	93%	85%	243

and channels were designed so that the pressure drop was the same for each, allowing for a passive fluid flow split.

Cell Line Selection. The L2 rat lung cell line was used to imitate the lung, a toxicity target tissue [6, 20]. L2 cells possess many of the characteristics of primary rat type II lung epithelial cells, including glutathione-*S*-transferase activity [21]. The HepG2/C3A cell line, which is a subclone of the HepG2 cell line, was used as a model for the liver. This cell line has detectable CYP1A and 2E1, UDP-glucuronyltransferase, sulfotransferase, and glutathione-*S*-transferase activity [22]. The Caco-2 cell line was used to mimic the intestinal epithelium. When seeded onto Type I collagen-coated inserts or culture plates under normal culture conditions, Caco-2 cells differentiate into a polarized, enterocyte-like epithelial barrier that is morphologically and biochemically very similar to the small intestinal epithelium [23]. After a growth period of two to three weeks, the Caco-2 monolayers express tightly packed microvilli, tight junctions, and are capable of paracellular, transcellular, active, and transcytotic transport [24]. Type I collagen is used to model the epithelial basement membrane because it has been found to best stimulate proliferation, cell spreading, and differentiation in static Caco-2 cultures [25]. Caco-2 cells also express CYP1A, 2E1, UDP-glucuronyltransferase, sulfotransferase, and glutathione-*S*-transferas [26-28].

CYP 1A and 2E1 Activity. The CYP1A and CYP2E1 activity of HepG2/C3A and Caco-2 cells was assessed using a fluorescent and colorimetric substrate, respectively (**Figure 4**). CYP2E1 activity is expressed as μM 4-nitrocatechol formation/mg cell protein/hr and CYP1A activity is expressed as μM resorufin formation/mg cell protein/hr. Both cell lines have detectable CYP1A and CYP2E1 activity under the culture conditions used for these experiments, although the values are much lower than those found in humans [22, 27].

μCCA Acetaminophen Toxicity. Culture medium with 30 mM APAP was pumped through the apical chamber of the GI tract μCCA for 6 hours. Culture medium without drug was pumped through the basolateral chamber of the GI tract μCCA and chip μCCA, therefore drug had to diffuse through the Caco-2 cell monolayer to reach the chip μCCA. After the 6 hour experiments, cells were stained with calcein and MCB to indicate viable cells and glutathione levels, respectively. Control experiments were run simultaneously without APAP in the GI tract μCCA apical chamber.

Figure 5A shows the cell viability results as a percent of control. The viability of HepG2/C3A cells decreased to 56% of the control and the viability of L2 cells decreased to 18% of the control. **Figure 5B** shows the cell glutathione levels as a percent of control. The HepG2/C3A glutathione levels decreased to 45% of the control and the L2 glutathione levels decreased to 10% of the con-

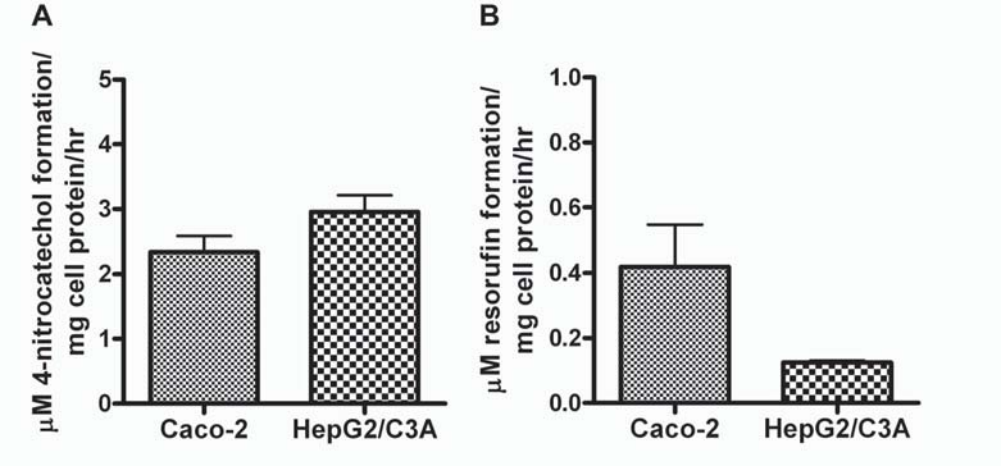

Figure 4: Metabolizing cell line CYP2E1 (A) and CYP1A (B) activity (n = 32).

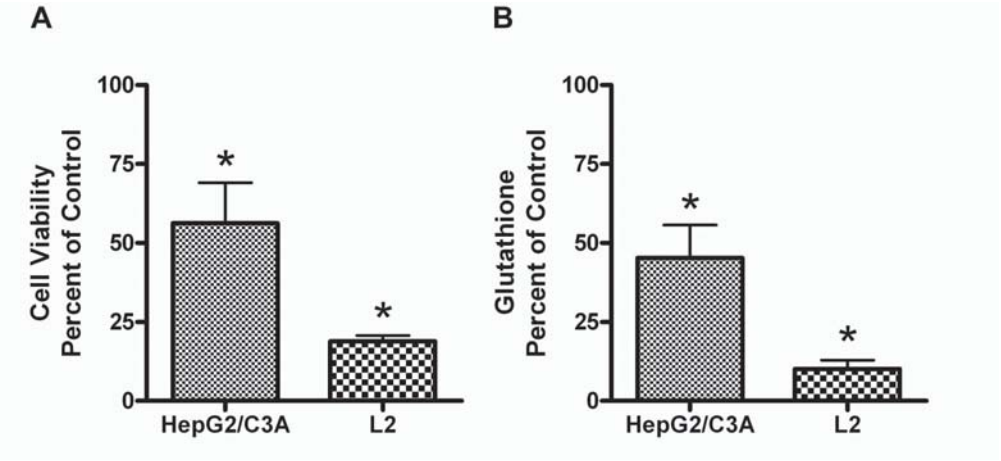

Figure 5: HepG2/C3A and L2 viability (A) and glutathione levels (B) after culture medium with 30 mM APAP was pumped through the apical chamber of the GI tract μCCA for 6 hours. Controls had only culture medium pumped through the apical GI tract μCCA chamber. Values are expressed as a percent of control $\pm$ SEM. Differences in viability or glutathione levels between cells exposed to APAP and controls that are significant according to an unpaired Student's t-test are indicated with a * ($p < 0.05$, n = 3).

trol. **Figures 6** shows the control (**Figures 6A and 6C**) and 30 mM APAP treated (**Figures 6B and 6D**) HepG2/C3A and L2 cells on the chip. The Caco-2 images were taken through 1/2 inch etched plexiglass, which did not allow for images that were of high enough quality for analysis. The Caco-2 cells were viable and the monolayers did remain intact in controls and after APAP exposure (data not shown).

HPLC analysis of the apical and basolateral GI tract μCCA culture medium revealed that the concentration of APAP in the basolateral chamber, and, therefore the medium circulating through the chip, reached 10 ± 2.6 mM. The culture medium in the apical chamber decreased from 30 mM to 13 ± 3.1 mM after the 6 hour experiment.

Experiments with only the chip μCCAs were run with DMEM/F12 +30 mM APAP recirculating for 6 hours. These experiments were done to determine the effects of adding the GI tract μCCA to the system. The result was 100% cell death for both HepG2/C3A and L2 cells (data not shown).

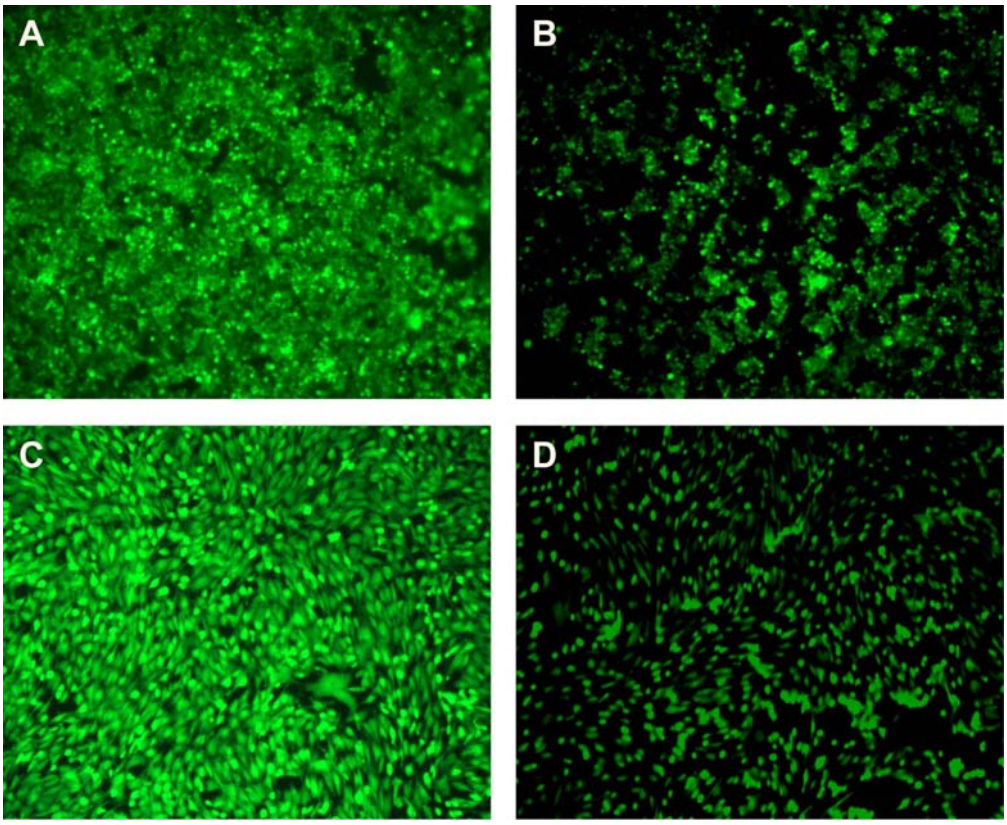

Figure 6: Comparison of control (A) and 30 mM APAP treated (B) HepG2/C3A cells and control (C) and 30 mM APAP treated (D) L2 cells on the chip μCCA after a 6 hour experiment where culture medium (control) or 30 mM APAP was pumped through the apical chamber of the GI tract μCCA.

4 Discussion

Oral delivery is the preferred route of pharmaceutical administration due to the relatively low medical costs and relatively high patient comfort, compliance and convenience; but the intestinal wall acts as a biological barrier that both limits the uptake of and biotransforms drugs [29, 30]. Biotransformation occurs during transcellular absorption when pharmaceuticals come in contact with phase I and phase II enzymes [31]. The most notable phase I enzymes belong to the cytochrome P450 superfamily which oxidize compounds, especially chemicals or drugs that are hydrophobic and relatively insoluble, to form a reactive intermediate [32]. The reactive intermediate is then susceptible to conjugation by a phase II enzyme such as UDP-glucuronyltransferase, sulfotransferase, or glutathione-*S*-transferase [31]. The resulting conjugate is almost always pharmacologically inactive and less lipid soluble than its precursor, allowing the conjugate to be excreted in bile or urine [32].

The membrane lining the small intestine is composed of two main cell types: enterocyte and goblet. Absorptive enterocytes make up about 90% of the cell population in the upper intestine, display very tight intracellular junctions (protein connections between epithelial cells that reduce passive diffusion between the cells), and are covered with 1 μm long, tightly packed projections called microvilli [33]. Microvilli further increase the surface area of the intestine available for absorption. The absorptive cells allow the passage of small molecules by one or more of four different routes: passive transcellular (through the cell), passive paracellular (between cells), active (energy-dependent) carrier-mediated and transcytosis (transport across the epithelium with uptake into coated vesicles) [34]. Any material that is

absorbed in the intestine must first diffuse across the mucus layer, the epithelial cells lining the intestine, the lamina propria, and the endothelial cells that line the capillaries, but the epithelial cell layer has been shown to be the rate-limiting step [35]. Caco-2 cells mimic absorptive enterocytes, which are the most populous cells in the intestinal epithelium. Caco-2 cells also develop tight junctions, possess microvilli, can transport small molecules by all four major transport routes, and express many phase I and phase II enzymes [24, 26, 27]. These qualities, along with the fact that epithelial cell layer has been shown to be the most significant barrier to oral absorption, make Caco-2 cells an appropriate model for oral absorption studies.

At a therapeutic levels APAP is generally considered safe, but high doses cause liver cell necrosis [36]. The liver toxicity is due to CYP bioactivation of APAP to a reactive metabolite, NAPQI [10]. The lung is one of the major targets for exposure to xenobiotics because it receives 100% of cardiac output, and in humans lung injury is a common result of APAP overdose [37, 38]. Studies with rat type II pneumocytes and alveolar macrophages suggest that CYP and/or prostaglandin synthetase are involved in APAP lung toxicity [39].

Here we describe a prototype *in vitro* system that for the first time, although at a very basic level, mimics oral exposure to a drug, first pass metabolism, and the circulation of metabolites on a microscale. These results demonstrate that APAP can cross the Caco-2 cell monolayer and damage cells in the liver and lung compartments. The GI tract μCCA minimizes the toxicity of the APAP dose and acts as a barrier, however, as 30 mM APAP running through only the chip μCCA resulted in 100% cytotoxicity and the final concentration of APAP in the chip μCCA run together with the GI tract μCCA was approximately 10 mM. The GI tract μCCA could be minimizing the toxicity in one or a combination of the following ways: the concentration of the APAP could quickly reach near-equilibrium between the two μCCAs, and the extra medium flowing through the GI tract μCCA could dilute the concentration to a less toxic concentration; the Caco-2 cells could metabolize some of the drug into harmless compounds, preventing some of the APAP from reaching the liver and lung compartments; and/or the Caco-2 monolayer may truly act as a barrier and the drug may slowly diffuse into the basolateral chamber.

The primary markers for cell toxicity in the μCCA system experiments were glutathione depletion and cell viability. After a 6 hour exposure to APAP approximately half of the liver cells remained, while only about 20% of the lung cells remained viable. The APAP dose was less toxic to the HepG2/C3A cells, which does not mimic *in vivo* results. The L2 cell line, however, expresses fewer phase II enzymes than the HepG2/C3A cell line. The viability results were most likely due to the increased phase II enzyme activity of HepG2/C3A cells when compared with the L2 cell line. The HepG2 cells were presumably able to detoxify a larger amount of APAP via the glucuronide and sulfation pathways. The glutathione levels in each cell compartment correlated with the number of viable cells remaining after the 6 hour APAP dose. Caco-2 cells remained viable and the monolayers remained intact after a 6 hour, 30 mM APAP exposure (data not shown).

The chip and GI tract μCCAs described here provide a framework for studying oral drug absorption and metabolism, but this system has several limitations. The chip was designed to mimic first pass metabolism in that all fluid circulating through the GI tract goes directly to the liver, but is diluted with fluid pumped directly to the liver. In order to achieve this effect two pump channels and two chip inlets were necessary. The peristaltic pump can only be run at a single flowrate, therefore the amount of medium pumped through the basolateral side of the GI tract μCCA was higher than desired and resulted in residence times that did not match physiological values. If the channel pumping to the basolateral chamber could have been run at 0.5 μL/min, for example, the residence times in the basolateral chamber and liver chamber would have been much closer to *in vivo* values. The two-inlet design of the chip and the addition of the GI tract μCCA made it very diffi-

cult to assemble and run the devices without letting air into the system. Air bubbles in the system often caused leakage and/or loss of cell viability [40], and experimental results from systems with an excessive amount of air bubbles had to be discarded. This issue with air bubbles necessitated the short experimental time frame (there were fewer problems with air bubbles during shorter experiments) and high drug concentrations (more physiologically relevant APAP concentrations did not have a noticeable effect on cells after only 6 hours).

Future experiments with the chip and GI tract μCCA system will incorporate several improvements. The chip will be designed with one inlet and outlet to reduce the amount of air that enters the system. This should allow for longer experiments and more physiologically realistic APAP concentrations. Goblet-like, mucus secreting cells will be incorporated into the GI tract μCCA membrane to better mimic the cell composition *in vivo*. HPLC will be used to determine the APAP and metabolite concentrations at different time points throughout the experiment. Finally, an *in vitro* digestion of APAP will be performed and this chyme mimic will be pumped through the apical chamber of the GI tract, better re creating the absorption conditions in the upper small intestine.

The μCCA system can overcome many of the drawbacks found in traditional drug testing methods. Multiple cell types and recirculating medium allow researchers to analyze the systemic effects of the compound being studied and the effects its metabolites. Human cells can be used in the μCCAs, offering a superior method for predicting a potential drug's effect on humans and sparing animals. The μCCAs are also inexpensive to produce and use very little of the compound of interest. The development and incorporation of a physiologically realistic GI tract μCCA may offer a better way to understand the kinetics of orally delivered drug ADMET, may aid in the development of oral delivery strategies, could help to find correct oral dosages for new pharmaceuticals, and might potentially better predict the systemic toxicity of orally delivered drugs.

Acknowledgement: This work was supported by the Nanobiotechnology Center (NBTC), an STC Program of the National Science Foundation, under Agreement No. ECS-9876771; the New York State Office of Science, Technology and Academic Research (NYSTAR) program through a grant to MLS as a NYSTAR Distinguished Professor; and Army Corp of Engineers under Agreement ID W9132T-07-2-0010.

References

1. DiMasi JA, Hansen RW, Grabowski HG. 2003. The price of innovation: New estimates of drug development costs. *Journal of Health Economics*. 22(2):151.

2. Agres T. 2005. Finding blockbusters a struggle. *Drug Discovery & Development*. 8(3):16-19.

3. Sankar U. 2005. The delicate toxicity balance in drug discovery. *The Scientist*. 19(15):32-34.

4. Brown RP, Delp MD, Lindstedt SL, Rhomberg LR, Beliles RP. 1997. Physiological parameter values for physiologically based pharmacokinetic models. *Toxicology and Industrial Health*. 13(4):407-484.

5. Sin A, Chin KC, Jamil MF, Kostov Y, Rao G, Shuler ML. 2004. The design and fabrication of three-chamber microscale cell culture analog devices with integrated dissolved oxygen sensors. *Biotechnology Progress*. 20(1):338-345.

6. Viravaidya K, Sin A, Shuler ML. 2004. Development of a microscale cell culture analog to probe naphthalene toxicity. *Biotechnology Progress*. 20(1):316-323.

7. Viravaidya K, Shuler ML. 2004. Incorporation of 3T3-L1 cells to mimic bioaccumulation in a microscale cell culture analog device for toxicity studies. *Biotechnology Progress*. 20(2):590-597.

8. Bessems JGM, Vermeulen NPE. 2001. Paracetamol (acetaminophen)-induced toxicity: Molecular and biochemical mechanisms,

analogues and protective approaches. *Critical Reviews in Toxicology*. 31(1):55-138.

9. Corcoran GB, Mitchell JR, Vaishnav YN, Horning EC. 1980. Evidence that acetaminophen and *N*-hydroxyacetaminophen form a common arylating intermediate, *N*-acetyl-para-benzoquinoneimine. *Molecular Pharmacology*. 18(3):536-542.

10. Patten CJ, Thomas PE, Guy RL, Lee MJ, Gonzalez FJ, Guengerich FP, Yang CS. 1993. Cytochrome-P450 enzymes involved in acetaminophen activation by rat and human livermicrosomes and their kinetics. *Chemical Research in Toxicology*. 6(4):511-518.

11. Mitchell JR, Jollow DJ, Potter WZ, Gillette JR, Brodie BB. 1973. Acetaminophen-induced hepatic necrosis. 4. Protective role of glutathione. *Journal of Pharmacology and Experimental Therapeutics*. 187(1):211-217.

12. Qiu YC, Benet LZ, Burlingame AL. 1998. Identification of the hepatic protein targets of reactive metabolites of acetaminophen *in vivo* in mice using two-dimensional gel electrophoresis and mass spectrometry. *Journal of Biological Chemistry*. 273(28):17940-17953.

13. Donato MT, Gomezlechon MJ, Castell JV. 1993. A microassay for measuring cytochrome-*P*450IA1 and cytochrome-*P*450IIB1 activities in intact human and rat hepatocytes cultured on 96 well plates. *Analytical Biochemistry*. 213(1):29-33.

14. Donato MT, Klocke R, Castell JV, Stenzel K, Paul D, Gomez-Lechon MJ. 2003. Constitutive and inducible expression of CYP enzymes in immortal hepatocytes derived from SV40 transgenic mice. *Xenobiotica*. 33(5):459-473.

15. Dicker E, McHugh T, Cederbaum AI. 1990. Increased oxidation of para-nitrophenol and aniline by intact hepatocytes isolated from pyrazole-treated rats. *Biochimica et Biophysica Acta*. 1035(3):249-256.

16. Bradford MM. 1976. Rapid and sensitive method for quantitation of microgram quantities of protein utilizing principle of protein-dye binding. *Analytical Biochemistry*. 72(1-2):248-254.

17. Kautzky F, Hartinger A, Kohler LD, Vogt H-J. 1996. *In vitro* cytotoxicity of antimicrobial agents to human keratinocytes. *Journal of the European Academy of Dermatology and Venereology*. 6(2):159-166.

18. Chai JN, Lu FZ, Li BM, Kwok DY. 2004. Wettability interpretation of oxygen plasma modified poly(methyl methacrylate). *Langmuir*. 20(25):10919-10927.

19. Wang EJ, Li Y, Lin M, Chen LS, Stein AP, Reuhl KR, Yang CS. 1996. Protective effects of garlic and related organosulfur compounds on acetaminophen-induced hepatotoxicity in mice. *Toxicology and Applied Pharmacology*. 136(1):146-154.

20. Hopkinson D, Bourne R, Barile FA. 1993. *In vitro* cytotoxicity testing - 24-hour and 72-hour studies with cultured lung cells. *ATLA-Alternatives To Laboratory Animals*. 21(2):167-172.

21. Shi MM, Kugelman A, Iwamoto T, Tian L, Forman HJ. 1994. Quinone-induced oxidative stress elevates glutathione and induces gamma-glutamylcysteine synthetase-activity in rat lung epithelial L2 cells. *Journal of Biological Chemistry*. 269(42):26512-26517.

22. Hewitt NJ, Hewitt P. 2004. Phase I and II enzyme characterization of two sources of HepG2 cell lines. *Xenobiotica*. 34(3):243-256.

23. Hidalgo IJ, Raub TJ, Borchardt RT. 1989. Characterization of the human-colon carcinoma cell-line (Caco-2) as a model system for intestinal epithelial permeability. *Gastroenterology*. 96(3):736-749.

24. Artursson P, Karlsson J. 1991. Correlation between oral drug absorption in humans and apparent drug permeability coefficients in hu-

man intestinal epithelial (Caco-2) cells. *Biochemical and Biophysical Research Communications*. 175(3):880-885.

25. Basson MD, Turowski G, Emenaker NJ. 1996. Regulation of human (Caco-2) intestinal epithelial cell differentiation by extracellular matrix proteins. *Experimental Cell Research*. 225:301-305.

26. Borlak J, Zwadlo C. 2003. Expression of drug-metabolizing enzymes, nuclear transcription factors, and ABC transporters in Caco-2 cells. *Xenobiotica*. 33(9):927-943.

27. Prueksaritanont T, Gorham LM, Hochman JH, Tran LO, Vyas KP. 1996. Comparative studies of drug-metabolizing enzymes in dog, monkey, and human small intestine cells, and in Caco-2 cells. *Drug Metabolism and Disposition*. 24(6):634-642.

28. Baranczykkuzma A, Garren JA, Hidalgo IJ, Borchardt RT. 1991. Substrate-specificity and some properties of phenol sulfotransferase from human intestinal Caco-2 cells. *Life Sciences*. 49(16):1197-1206.

29. Lee HJ. 2002. Protein drug oral delivery: The recent progress. *Archives of Pharmaceutical Research*. 25(5):572-584.

30. Lampen A, Bader A, Bestmann T, Winkler M, Witte L, Borlak JT. 1998. Catalytic activities, protein- and mRNA-expression of cytochrome P450 isoenzymes in intestinal cell lines. *Xenobiotica*. 28(5):429-441.

31. Doherty MM, Charman WN. 2002. The mucosa of the small intestine: How clinically relevant as an organ of drug metabolism? *Clinical Pharmacokinetics*. 41(4):235-253.

32. Rang HP, Dale MM, Ritter JM. 1999. Pharmacology. 4th ed. Edinburgh: Churchill Livingston.

33. Forstner JF, Forstner GG. 1994. Gastrointestinal mucus. Johnson LR, editor. Physiology of the gastrointestinal tract, 3rd ed. New York: Raven Press.

34. Artursson P, Palm K, Luthman K. 2001. Caco-2 monolayers in experimental and theoretical predictions of drug transport. *Advanced Drug Delivery Reviews*. 46(1-3):27-43.

35. Audus KL, Bartel RL, Hidalgo IJ, Borchardt RT. 1990. The use of cultured epithelial cells for drug transport and metabolism studies. *Pharmaceutical Research*. 7(5):435-451.

36. Mitchell JR, Jollow DJ, Potter WZ, Davis DC, Gillette JR, Brodie BB. 1973. Acetaminophen-induced hepatic necrosis. 1. Role of drug-metabolism. *Journal of Pharmacology and Experimental Therapeutics*. 187(1):185-194.

37. Dimova S, Hoet PHM, Nemery B. 2001. Xenobiotic-metabolizing enzyme activities in primary cultures of rat type II pneumocytes and alveolar macrophages. *Drug Metabolism and Disposition*. 29(10):1349-1354.

38. Baudouin SV, Howdle P, Ogrady JG, Webster NR. 1995. Acute lung injury in fulminant hepatic-failure following paracetamol poisoning. *Thorax*. 50(4):399-402.

39. Dimova S, Hoet PHM, Nemery B. 2000. Paracetamol (acetaminophen) cytotoxicity in rat type II pneumocytes and alveolar macrophages *in vitro*. *Biochemical Pharmacology*. 59(11):1467-1475.

40. Sin A, Reardon CF, Shuler ML. 2004. A self-priming microfluidic diaphragm pump capable of recirculation fabricated by combining soft lithography and traditional machining. *Biotechnology and Bioengineering*. 85(3):359-363.